WAVE PRESSURE DISTRIBUTION ON PERMEABLE VERTICAL WALLS

Hendrik Bergmann[1], Hocine Oumeraci[2]

Abstract

The pressure distribution at permeable vertical walls is investigated within a comprehensive large-scale test programme considering experiments with a variation of wave parameters and structure porosities. Monochromatic non breaking and slightly breaking waves on such structures are examined and results are compared to the GODA formula for impermeable vertical walls and a modified GODA method which has been developed here for permeable walls. Two parameters involving the structure porosity are introduced to account for the nonlinear processes at permeable walls. Using these parameters new prediction formulae have been derived for the pressure distribution at the wall.

1. Introduction

The advantages of permeable vertical wave barriers are obvious in terms of wave damping performance, reduction of wave reflection, overtopping and forces. Wave damping is of fundamental importance for the protection of harbours and marinas. Rubble mound structures can be used if there are no limitations in space and in case of shallow water depth, otherwise vertical structures may be favoured. However, impermeable vertical structures result in considerable wave reflection which can cause navigation problems in harbour entrances for smaller vessels. Therefore, it might be advisable to use perforated structures which allow to better control wave transmission and reflection. In this case reliable information on wave loads and pressure distribution on the permeable wall is needed for stability analysis and design.

The most widely used pressure formulae for the design of coastal structures with vertical walls under breaking and non breaking wave conditions are the GODA

---

[1] Dipl.-Ing., Research Assistant, Leichtweiss-Institut, TU Braunschweig, Beethovenstr. 51a, 38106 Braunschweig, Germany, e-mail: h.bergmann@tu-bs.de

[2] Prof. Dr.-Ing., University Professor, Managing Director of Leichtweiss-Institut, TU Braunschweig

formulae (1985). However, these formulae do not account for a wall porosity so that reduction coefficients can only be estimated by engineering experience or obtained from hydraulic model tests. Therefore, the hydraulic performance and the pressure distribution of single permeable vertical walls was investigated within a comprehensive large-scale test programme. The extension of the existing formulae in terms of structure permeability was performed considering experiments in intermediate water depth with different wave conditions and structure porosities. For this paper only non breaking and slightly breaking waves on such structures were examined and results are compared to the GODA method for impermeable walls. Two dimensionless parameters involving the structure porosity were introduced to account for the nonlinear processes at permeable walls.

2. Experimental Set-up and Test Conditions

The tests were conducted in the Large Wave Flume (GWK) of the Coastal Research Centre, a joint institution of the University of Hannover and the Technical University of Braunschweig. The flume has a length of 320m, a width of 5m and a depth of 7m (Fig. 1). A sand beach with a slope of 1:6 was installed about 220m from the wave paddle for the dissipation of transmitted wave energy. The vertical permeable wall, made of horizontal steel bars was located about 100m from the wave paddle.
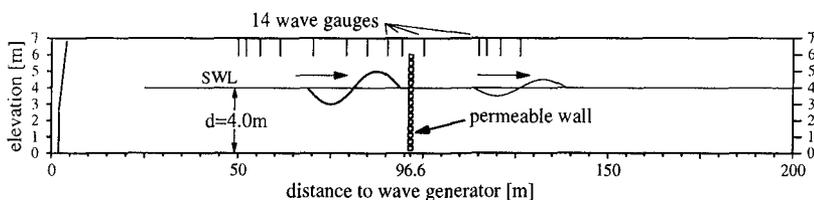
Figure 1: Cross Section of the Large Wave Flume (GWK)
with Positions of Permeable Wall and Wave Gauges.

The incident waves, wave transmission and wave reflection were analyzed by wave gauges which were grouped in three harps (one in the far field, one in front and one behind the structure) with 4 wave gauges each. Additional wave gauges were installed to measure the water surface elevation and the waterlevel gradient directly at the permeable wall.

The tests were carried out with regular waves (H=0.5-1.5m and T=4.5-12s), random waves (H_s=0.5-1.25m, T_p=4.5-12s), solitary waves (H=0.5-1.0m) and transient wave packets. The water depth was kept constant (d=4.0m) in the test phase with permeable walls but was varied between 3.25 and 4.75m for the impermeable wall tests (P=0%). Due to the structure height of approximately 6m, overtopping is negligible.

The structure porosity P=s/e, with gap spacing s and distance e between two ad-
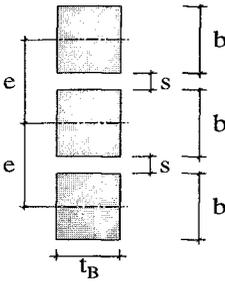
Figure 2: Definition of
Structure Porosity P=s/e.

jacent element axis' (Fig. 2), was varied in five steps: P=0.0% (impermeable wall), 11%, 20%, 26.5% and 40.5%. A permeable wall consists of up to 29 horizontal elements which were built of quadratic steel pipes ($t_B \times b$: 180×180mm, Fig. 2). The tested structures had an overall weight of up to eight tons depending on their porosity.

In order to analyze the resulting wave loads pressure transducers of type NATEC SCHULTHEISS PDCR 830 were installed at 10 positions at the front and rear side of the structure. Fig. 3 shows the front view of the wall (porosity P=26.5%) with locations of the pressure transducers over the structure height. The resultant pressures were calculated by adding the two pressure components on both sides of the wall elements which were equipped with pressure cells (Fig. 4). Data were recorded at 200Hz logging frequency.
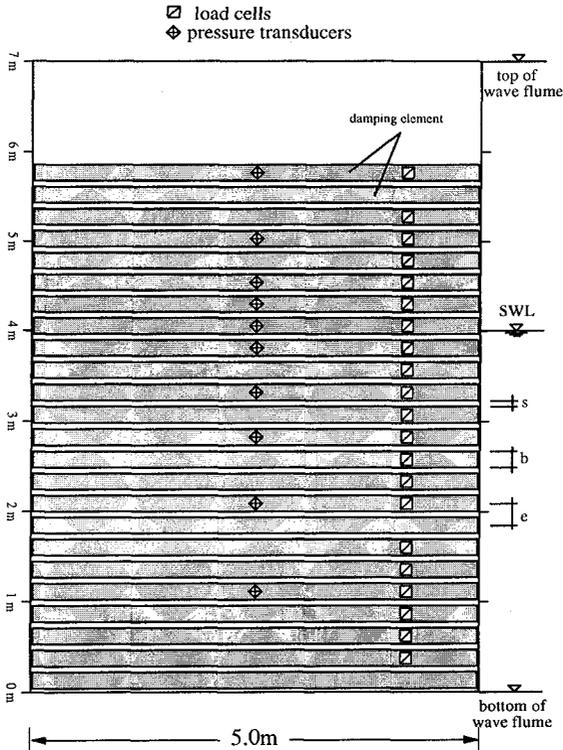
Figure 3: Locations of Pressure Transducers and Load Cells for a Permeable Wall with Porosity P=26.5%.

wall element 180x180 mm
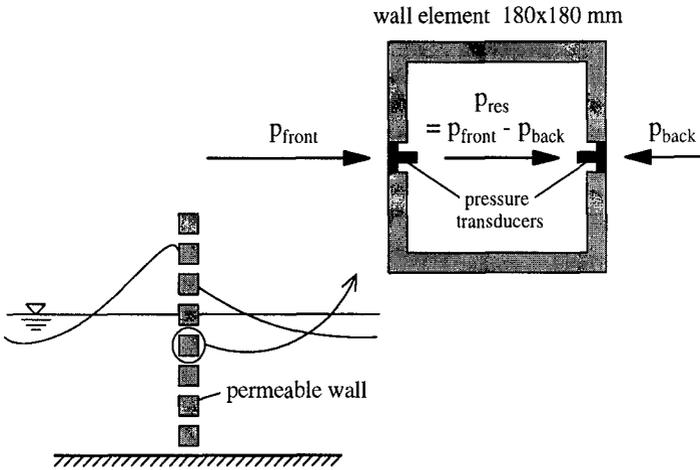
Figure 4: Calculation of Resultant Pressures p_{res}.

3. Experimental Results and Discussion

The hydrodynamic pressure distribution under wave attack at the front of a vertical impermeable structure can be described by the water surface elevation η^* above still water level, the pressure p_1 at still water level (SWL) and the pressure p_2 at the toe of the structure (GODA, 1985). For the vertical walls tested in the GWK (2D-case, normal incidence of waves, no berm) the equations for the characteristic values (Fig. 5) described by GODA can be simplified to:
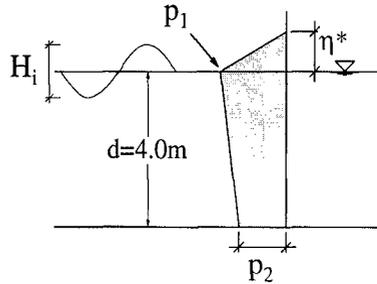
Figure 5: Definition Sketch for Pressure Distribution according to GODA's Method.

$$\eta^* = 1.5 \cdot H_i \tag{1}$$

$$p_1 = \alpha_1 \cdot \rho \cdot g \cdot H_i \tag{2}$$

with $\alpha_1 = 0.6 + 0.5 \cdot \left(\dfrac{(4\pi d/L)}{\sinh(4\pi d/L)} \right)^2$ \hfill (3)

$$p_2 = \frac{1}{\cosh(2\pi d/L)} \cdot p_1 \hfill (4)$$

The tests considered in this paper were run with monochromatic waves. The wave height H_i describes the mean incident wave height and L is the local wave length at the structure.

Fig. 6 shows the measured pressure heads at the front and at the rear side for different structure porosities. Results are shown exemplarily for an incident wave height of H_i=0.80m and a wave period of T=8s for all porosities investigated. In addition, the calculated pressures (Eq. (1) - Eq. (4)) on an impermeable wall are also plotted. The graph represents a) the pressure distribution acting simultaneously on the front face of the wall and on the rear side of the wall (left side) and b) the resultant pressures (right side) for the time step where the maximum total force on the structure occurred (wave crest). The total horizontal force was obtained by integration of measured resultant pressures over the structure height for every time step.
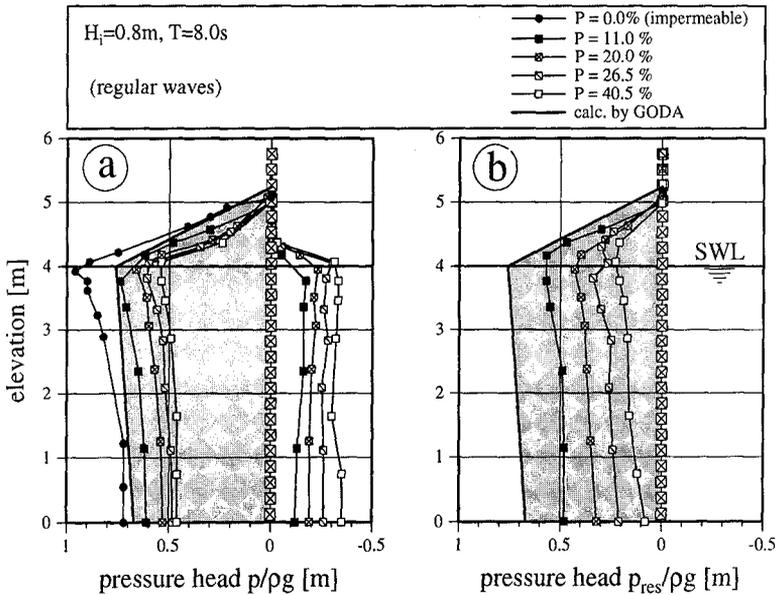
Figure 6: Simultaneous Pressure Distribution on Front and Back Side (a) and Resulting Pressure Distribution (b).

Generally, all measurements show a similar profile compared to the GODA distribution, but the influence of the wall porosity is obvious. At the structure front

face higher pressures p_1 are observed for low structure porosities (P=11%), whereas on the rear side of the structure the higher pressures occur for large values of structure porosity (P=40.5%). Due to the reduction of pressure at the structure face and the increase of pressure at the rear side of the structure the resulting pressure values are even more reduced when compared to the calculated pressures for an impermeable wall (Fig. 6, right). Hence, in the case of a permeable wall the resulting pressure values $p_{1,res}$ and $p_{2,res}$ are the governing pressures for the calculation of the total loading of the structure. The resulting pressure values are calculated as described above (see also Fig. 4) and used for further analysis. In addition it is apparent from Fig. 6 that the wave run-up at the structure is overestimated by Eq. (1). In the following the aforementioned characteristic values will be discussed in terms of the porosity of the wall.

3.1   Maximum Surface Elevation at Structure Front η^*

The linear relationship between run-up height and wave height (Eq. (1)) is not appropriate for the description of the physical processes at the structure face. In fact, ratios η^*/H_i measured in the Large Wave Flume varied between 0.56 and 1.32 for P=40.5% to P=0.0%, respectively. The maximum wave run-up at the structure front (η^*) is governed by the influence of shallow water depth (function of d/L) and the reflection properties of the structure which is directly related to the reflection coefficient C_r and the structure porosity P. The influence of the structure porosity P is considered by the reduction parameter Ψ_e. The surface elevation at the structure face can be determined as:

$$\eta^* = \Psi_e \cdot \left[2 - \tanh\left(\frac{4\pi d}{L}\right) \right] \cdot H_i \tag{5}$$

where the reduction parameter Ψ_e is defined as a function of the wall porosity P:

$$\Psi_e = \left(1 - 0.5 \cdot \sqrt{P} \right) \tag{6}$$

The correlation between measured and calculated η^*-values is relatively good, although the wave run-up at the structure is slightly overestimated for small waves but underestimated for large waves (Fig. 7). This nonlinear process in terms of the wave height and the influence of the reduction parameter Ψ_e will be discussed more thoroughly under Section 3.2.2.

3.2   Pressure Distribution at Structure

In Fig. 8 all measured resultant pressure values $p_{1,res}$ (at SWL) under different wave conditions (regular waves) are shown in comparison with results using the GO-DA formula for impermeable walls. The influence of the structure porosity is significant, resulting in twice the $p_{1,res}$-values for the porous wall with a porosity P=11% as
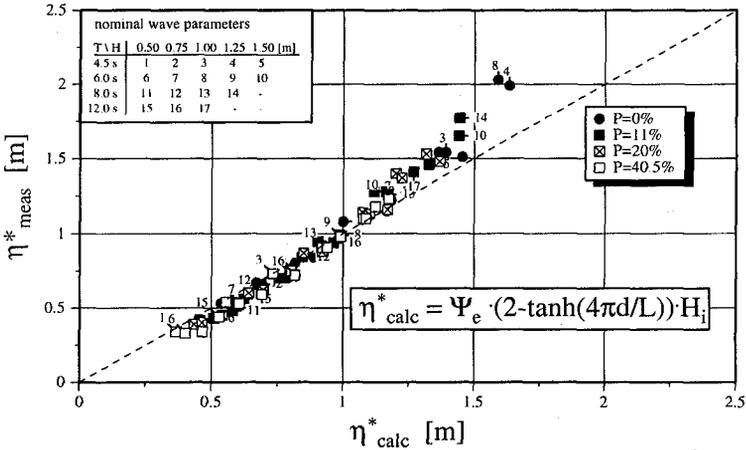
Figure 7: Measured and Calculated Maximum Surface Elevations η^* (Eq.(5)) at the Front Face of the Structure.

compared to a wall with porosity P=40.5%. The GODA formula overestimates the measured pressure values, mainly due to the influence of structure porosity.

It is also seen from Fig. 8 that the results for the impermeable wall tested in the GWK are not well predicted by the GODA formula. The measured pressures at SWL are underestimated, particularly for the longer waves (i.e. no. 11 - 17).
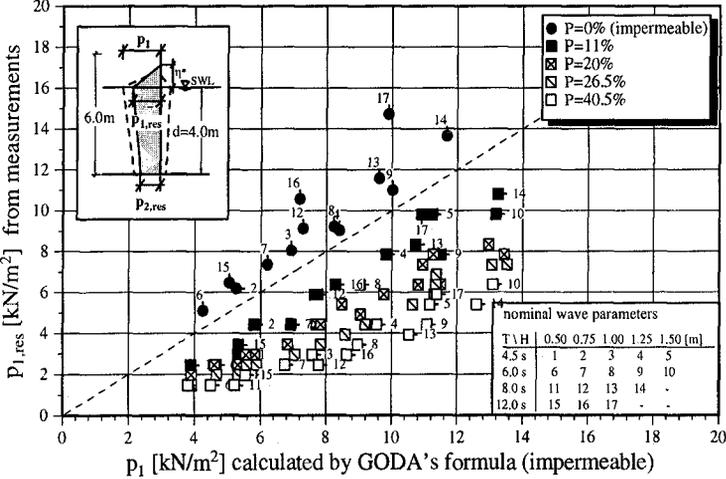
Figure 8: Comparison of Measured Pressure $p_{1,res}$ at SWL for Different Structure Porosities and Calculated Pressure p_1 for Impermeable Walls.

Applying a linear correction factor which accounts for the structure porosity of the permeable wall did not show satisfactory results. Smaller pressures $p_{1,res}$ are described accurately with this linear correction method while higher pressures are underestimated.

Hence, a correction procedure accounting for the load reduction due to porosity for vertical breakwaters in the GODA method has to consider nonlinear effects due to shallow water conditions and large wave heights. Consequently, the extension of the existing formulae has to be performed in two successive steps:

1. Modification of the GODA formula (Eqs. (2) and (3)) to predict the measured pressures in the reference case (impermeable wall).

2. Introduction of reduction factors considering the porosity of the structure.

3.2.1 Modification of the α_1-Value in the GODA Formula for the Impermeable Case

The normalised pressure p_1 at still water level in the simplified GODA formula (Eq. (2)) is controlled by α_1 which accounts for the maximum surface elevation at the structure

$$\alpha_1 = \frac{p_1}{\rho \cdot g \cdot H} = \left[0.6 + 0.5 \cdot \left(\frac{(4\pi d/L)}{\sinh(4\pi d/L)} \right)^2 \right] \tag{7}$$

Plotting α_1 as calculated by Eq.(7) over the relative water depth d/L, it becomes apparent that Eq.(7) does not represent the measured normalized pressures (Fig. 9).
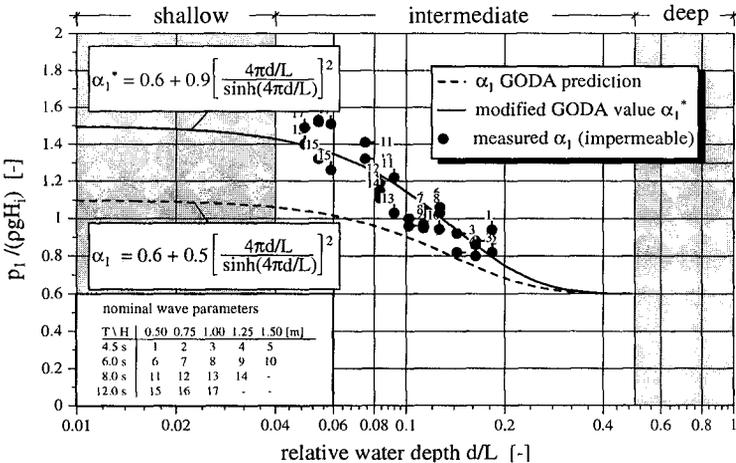
Figure 9: Normalized Pressure at SWL vs. the Relative Water Depth d/L.

Increasing the second coefficient for calculating α_1 from 0.5 to 0.9 allows a much better prediction of the data measured at the impermeable wall. This result seems to be acceptable as a first attempt to consider the influence of shallow water depth (tests performed in the region of shallow water to intermediate water depth, $0.04 < d/L < 0.5$, see Fig. 9). This modification has to be considered for the calculation of the resultant pressure at the structure toe $p_{2,res}$ which is described in Section 3.2.3.

3.2.2   Reduction Factors for Resultant Pressure at Still Water Level (SWL)

Moreover, besides modifying the GODA formula in terms of prediction of maximum pressures at impermeable structures the next step is to consider the force reduction due to the structure porosity. The reduction factors Ψ_p is introduced which describes the influence of the surface elevation at the rear side of the structure. The whole set of extended formulae regarding to maximum resultant pressure at SWL ($p_{1,res}$) are given as follows:

$$p_{1,res} = \rho \cdot g \cdot H^* \tag{8}$$

with

$$H^* = \alpha_1^* \cdot \Psi_e \cdot \Psi_p \cdot H_i \tag{9}$$

The resultant pressure head $p_{1,res}$ is controlled by the pressure gradient at the structure which is affected by the following factors

· the modified α_1-value in the GODA formula

$$\alpha_1^* = 0.6 + 0.9 \cdot \left(\frac{(4\pi d/L)}{\sinh(4\pi d/L)} \right)^2 \tag{10}$$

· reduction of wave run-up due to structure porosity (Ψ_e, Eq. (6))

· reduction of resulting pressure due to surface elevation at the back side of the structure

$$\Psi_p = \left(1 - \sqrt{P} \right)^a \qquad \text{with a} = \sqrt{\frac{1}{6} \frac{d}{H_i}} \tag{11}$$

The coefficient Ψ_e (Eq. (6)) is dependent on the structural porosity and describes the influence of the permeability on the wave run-up at the structure face. Ψ_p estimates the decrease in resulting pressure due to surface elevation at the back side of the structure (see also Fig. 6). Ψ_p is strongly influenced by the transmission of wave energy through the structure gaps which depends on the flow resistance induced by the velocity in the apertures. The schematic flow pattern is illustrated in Fig. 10. High waves and thus large horizontal velocity components increase the flow resistance due to large velocities in the structure gaps. Hence, for large wave heights the transmission of wave energy through the structure openings is much more limited compared

to small wave heights. The parameter Ψ_p describes therefore a kind of "dynamic porosity" of the structure. The expected influence of the wave period on wave transmission and flow resistance could not confirmed by the data.
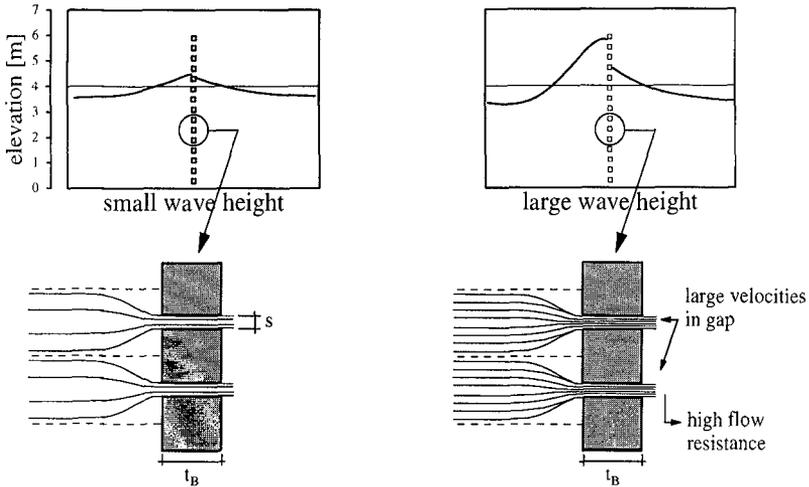
Figure 10: Flow Resistance for Small- (left) and Large Wave Heigths (right), Induced by the Velocity Gradients in the Structure Gaps.

In Fig. 11 the product of the two coefficients Ψ_e and Ψ_p is shown as a function of the wave height H_i for various structure porosities. For an impermeable wall no reduction of pressure values results from the equations given ($\Psi_e \cdot \Psi_p = 1$). In this case only the modification of the α_t^*-value should be considered for the prediction of the maximum resulting pressures at still water level. The reduction factors decrease significantly with increasing structure porosity which is even more relevant for smaller wave heights H_i.

3.2.3   Reduction Factors for the Resultant Pressure at the Structure Toe

Compared to impermeable walls, the pressure reduction at the structure toe is larger for permeable structures. This is due to the almost constant pressure over the water depth on the rear side of the structure (see Fig. 6). The main influencing parameter is the "dynamic porosity" (Ψ_p) which is therefore included in the depth dependent term of the GODA formula (see Eq.(4)). This will decrease the pressure $p_{2,res}$ at the structure toe. Additionally, a further reduction factor (85%) was necessary to fit the measured data (Eq.(12)). The following relation for $p_{2,res}$ was found:
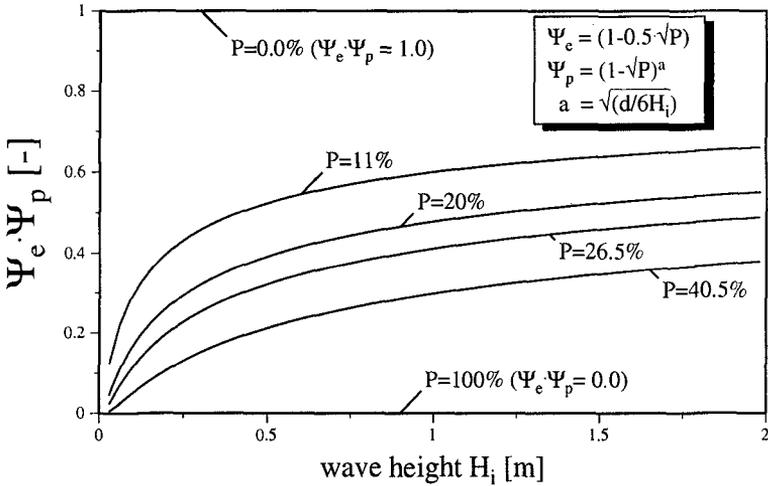
Figure 11: Total Reduction Coefficients Ψ_e and Ψ_p
versus Incident Wave Height.

$$p_{2,res} = 0.85 \cdot \frac{1}{\cosh\left(\dfrac{2\pi d}{L} \cdot \dfrac{1}{\Psi_p}\right)} \cdot p_{1,res} \tag{12}$$

Taking into account the modified α_1^* value and the reduction coefficients Ψ_e and Ψ_p the comparison of measured and calculated characteristic resulting pressure values $p_{1,res}$ and $p_{2,res}$ is shown in Fig. 12 and Fig. 13, respectively.

The results confirm the proposed formulae for the prediction of characteristic pressure values at permeable walls for maximum horizontal forces under wave crests.

3.3   Relation between Wave Elevation and Pressure Distribution at Permeable Walls

For the impermeable wall the wave elevation at the structure front η^* should result in the same value as the wave height H^* used for the calculation of resultant pressures. This is more or less verified by the data (Fig. 14, P=0%). For permeable vertical walls the ratio H^*/η^* is influenced by the surface elevation at the rear side of the structure and can be described by a factor $(1-P^{0.5})$.
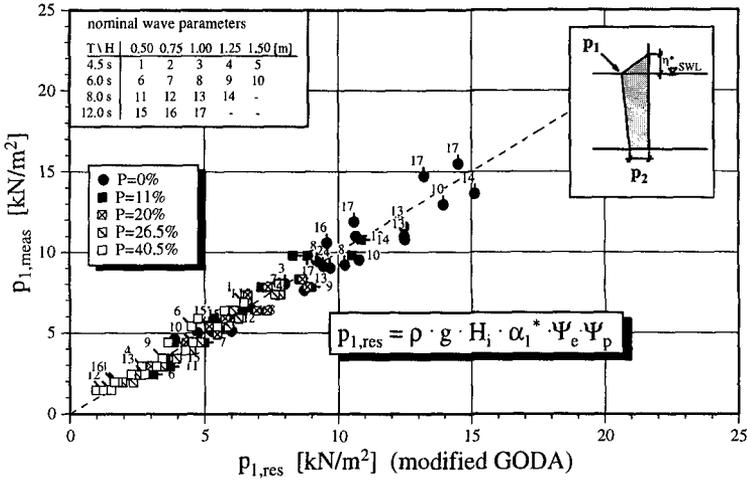
Figure 12: Measured and Calculated Resultant Pressures $p_{1,res}$ at SWL Considering the Nonlinear Influence of the Structure Porosity.
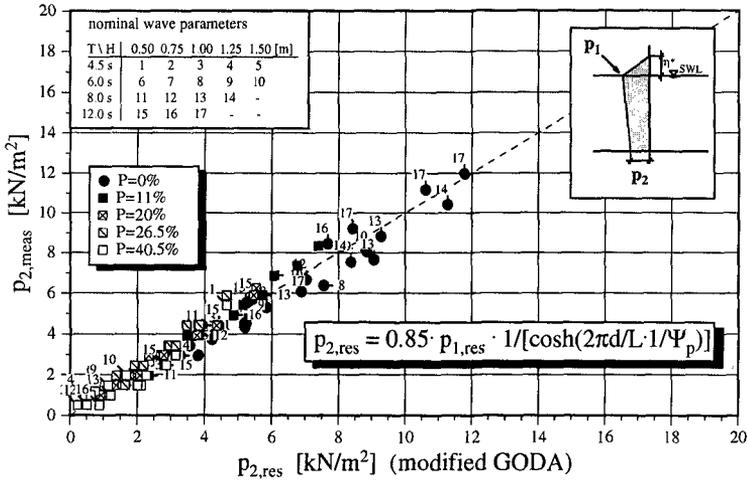
Figure 13: Measured and Calculated Resultant Pressures $p_{2,res}$ at Structure Toe Considering the Nonlinear Influence of the Structure Porosity.
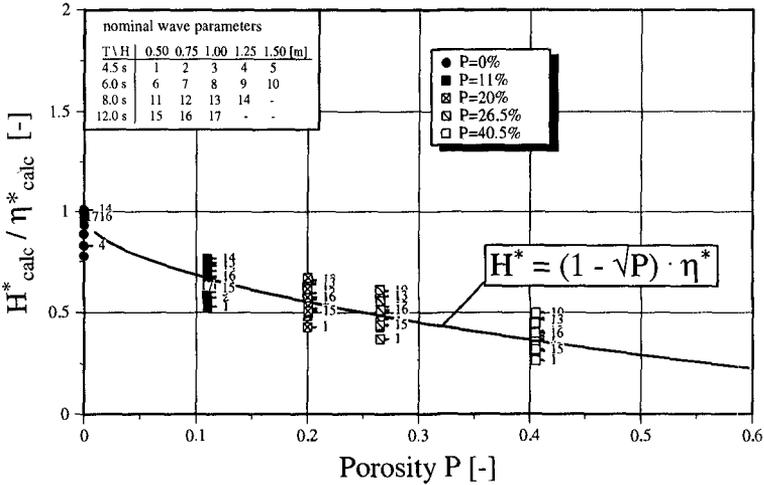
Figure 14: Ratio of Calculated Parameters for the Pressure Head at SWL (H^*) and Wave Elevation (η^*) as a Function of Structure Porosity.

The elevation of the nonlinear wave crest is described for the wave run-up by Eq. (5) and for the pressure distribution by Eq. (10). This should be done in a more consistent way by one equation. As a first attempt the resultant pressures on permeable walls should be calculated by the modified formulae (Eq. (6) -(12)). The elevation above still water level η^* estimated by Eq. (5) can be used as the upper limit of pressure integration for the calculation of horizontal forces.

It will be the objective of further studies to relate the resultant pressures directly to the nonlinear wave elevation at the structure front.

4. Conclusions and Future Work

For the design of permeable structures reliable information on wave loads and pressure distribution is needed. The influence of the incident wave height H_i, described by the "dynamic porosity" has to be considered for the analysis of wave damping processes at the porous wall. The resultant pressure distribution at vertical wave screens under non breaking and slightly breaking waves is dominantly governed by:

· the non-linear wave profile (section 3.2.1)

· reduction of wave run-up due to "structural porosity" (section 3.2.2)

· reduction of resulting pressure due to "dynamic porosity" (section 3.2.2)

The nonlinear extension of the GODA formulae for calculating the resultant pressure distribution at permeable vertical walls as proposed in this paper gives accurate results for wall porosities between 0% and 40.5%, as compared to data obtained from hydraulic model tests in the Large Wave Flume (GWK) of the Coastal Research Centre, Germany.

The future work will resolve the following main objectives:

· Pressure distribution under wave troughs

· Wave spectra (random conditions at front and rear side of the structure!)

· Chamber systems (combinations of different permeable walls followed by an impermeable wall).

5. Acknowledgements

6. References

GODA, Y. (1985) Random Seas and Design of Maritime Structures. University of Tokyo Press.